5-2014

Experimental and Simulation Studies of the Permeation of Water through Polydimethylsiloxane (PDMS)

Dilawer Singh
University of Arkansas, Fayetteville

This thesis is approved.

Thesis Advisor:

Thesis Committee:

David Jensen

Jerry Roe

Experimental and Molecular Simulation Studies of the Permeation of Water through Polydimethylsiloxane (PDMS)

An Undergraduate Honors College Thesis

in the

Department of Mechanical Engineering
College of Engineering
University of Arkansas
Fayetteville, AR

by

Dilawer Singh

Acknowledgments

I would like to express my gratitude to Dr. Douglas Spearot from the Mechanical Engineering Department and Dr. Gay Stewart from the Department of Physics for their continuous support and guidance throughout my thesis research. I would like to thank the High Performance Computing Center at the University of Arkansas for allowing me to use their computers for my work. I would also like to thank the Mechanical Engineering and Physics Departments for their help in offering me the resources to complete my thesis.

Table of Contents

Abstract

Experimental and computational techniques were used to test the permeation of water through polydimethylsiloxane (PDMS). The experimental portion consisted of creating a permeation cell in such a way that water's only path to escape was through a PDMS membrane. Weight measurements were recorded and turned into a permeation coefficient of water through different types of PDMS. The membranes were then stretched to a certain amount to study the effect on water permeation. The computational part used Large-scale Atomic / Molecular Massively Parallel Simulator (LAMMPS) to study the diffusion coefficient of water through PDMS. The initial step was to translate coarse-grain water model parameters into LAMMPS so that water could be accurately modeled. The next process involved calculating and including the parameters for both water-PDMS interaction sites and PDMS-PDMS interaction sites. Three restart files, differing in random numbers in the code, were used to create input files for the molecular dynamics simulations. Each restart file was used to produce 3 input files at 3 different temperatures, 200K, 300K, and 400K, creating a total of 9 simulations. The 300K file was put under 3 different pressures, 50 atm, 100 atm, and 150 atm, to mimic the PDMS under stretch /strain. The simulations would provide insight into diffusion-stretch correlation. The 100 atm file was run at 200K and 400K also to test temperature dependence with strain on the PDMS.

Introduction

Polydimethylsiloxane Formula

Polydimethylsiloxane is a clear, silicon-based organic polymer, and because of its distinctive properties, PDMS is commonly used in microfluidic and optical applications [1]. PDMS is a series of linear siloxane polymers of the repeating formula $(CH_3)_2SiO$. The linear chains begin and end with trimethylsiloxy ($(CH_3)_3SiO$-) units, and there is flexibility in the length of a chain which is characterized by the complete chemical formula of $CH_3[Si(CH_3)_2O]_nSi(CH_3)_3$, as shown in Figure 1.

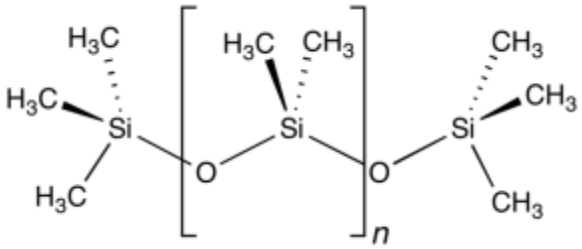

Figure 1: Polydimethylsiloxane Chemical Structure [2].

The *n* represents the number of the repeating monomer. A typical value of *n* is between 90 and 140 which leads to a molecular weight ranging from 6,800 to 30,000 g/mol [3].

PDMS Properties

The synthesis of PDMS can occur in one of two ways. One way is by mixing a viscous base with a viscous cross-linking agent (often methyltrichlorosilane) that initiates the cross-linking process without any additional aid, although it is greatly accelerated with heat. The other way is by creating PDMS without any cross-linking which is the base without any cross-linking agent. Cross-linked PDMS behaves as a rubbery solid that maintains its

configuration when put under stress or strain. The rubber elasticity of cross-linked PDMS depends on the amount of methyltricholorosilane that is added in the mixing process. Increasing the cross-linking agent yields a more rigid PDMS solid. Rather than a solid, PDMS without cross-linking will remain a viscous liquid, although for large molecular weights chain entanglements can lead to solid-like behavior. Regardless of PDMS linking, its chemical properties are the same. It is chemically inert and it is hydrophobic. However, diffusion of water through PDMS does occur under certain conditions [1]. It is also a clear solid or a clear liquid depending on its linking with a density slightly less than that of water ($0.91\ g/cm^3$) [4].

Applications of PDMS

The uses of PDMS are far-reaching and depend greatly on the amount of cross-linking. As a solid, PDMS has numerous uses in medical devices and pharmaceutical applications. Because it is composed mainly of silicone, liquid PDMS and PDMS-based elastomers are highly biocompatible because they are nonirritating and nonsensitizing to the human body [5]. For example, they are used in pacemakers, hydrocephalic shunts, and bioadhesives [6]. Also, PDMS is optically clear for a large range of wavelengths, so it has recently been used to form lenses and waveguides. Its effective refractive index and absorption spectrum are altered when organic compounds are physically absorbed by the polymer, establishing itself as the basis for many fiber-optic based chemical sensors [1].

Objective

The objective of this research is to study the permeation and diffusion of water through PDMS. The experimental aspects of this work to study permeation were conducted at the Harvard School of Engineering and Applied Sciences as part of a Research Experiences for Undergraduates program in material science. Simulations to study diffusion were performed in the Institute for Nanoscale Materials Science at the University of Arkansas using supercomputers in the Arkansas High Performance Computing Center. Permeation of water through PDMS has been studied thoroughly, but diffusion has been ignored because it was not relevant to traditional applications of PDMS, such as in microfluidic devices [7]. Since adaptive lenses have become more popular, especially with the use of dielectric elastomers, water diffusion through PDMS is beginning to be studied. Experimental results are hard to obtain because it is difficult to design an apparatus that measures only water diffusion through PDMS, eliminating the two other processes of permeation (absorption and desorption). With molecular dynamics, it is possible to computationally study and compute the diffusion coefficient, D, of water through PDMS. By varying the temperature, the activation energy, E_a, and the temperature-independent pre-exponential, D_0, will be calculated [8].

Experimental Research

Motivation

In all cameras today, the lens is focused onto the object's field of view by either moving the lens towards or away from the object in small increments. Typically, this movement is carried out by a set of gears that manually move the lens when the user either zooms in or

out. The same method is applied to keep the lens steady for the picture to be taken. This steadiness is a result of the gears constantly moving in opposition to the external vibrations to wholly cancel them out. Thus, cameras can take pictures when the user is in motion without any effect on the picture. However, a major flaw in this design is the way the lens is focused onto an object and how it is kept steady. Dielectric elastomers can help solve this problem. Dielectric elastomers are a group of electroactive polymers that experience large (>100%) deformations when a high electric field is applied to an elastomeric membrane [9], as shown in Figure 2.

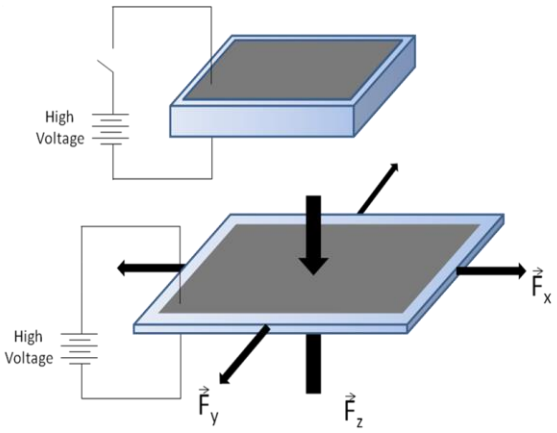

Figure 2: Electrostatic compression of an elastomer sheet results in large strains [10].

Using dielectric elastomers on either side of a gasket to encapsulate a clear liquid, an adaptive lens can be made. Such an adaptive lens is shown in Figure 3.

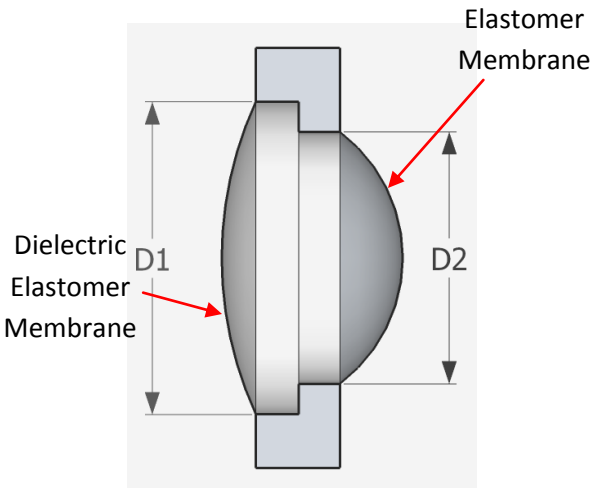

Figure 3: Schematic cross-section of an adaptive lens [11].

A major problem with the adaptive lens is that over time, the cavity liquid permeates through the membrane, degrading the lens performance [11]. Several different elastomers are thus evaluated to understand how chemical and physical properties affect the permeation coefficient. Experiments were focused entirely on quantifying the amount of water permeating through each membrane as to give some understanding on which is the best permeation barrier.

Experimental Setup

After preparing the elastomer films through doctor blading and curing, the first task was to construct a suitable permeation cell. The procedure employed a modified American Society for Testing and Materials (ASTM) standard E96-80 for measuring permeation of water through elastomer membranes. After some preliminary designs, the final device was constructed that would act as a permeation cell. The schematic of the design is shown in Figure 4.

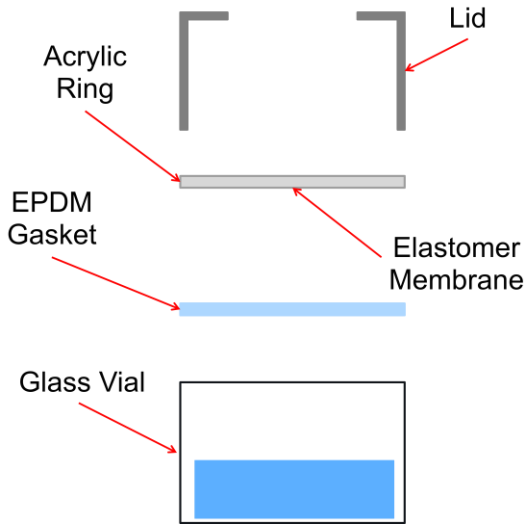

Figure 4: Basic schematic of the permeation cell used to conduct experiments.

The design of the ethylene propylene diene monomer (EPDM) gasket ensured a tight seal between the membrane, acrylic ring, and glass vial. The cell was then filled with drierite, which is made of calcium sulfate. The permeation cell prior to testing is shown in Figure 5.

Figure 5: Permeation cell prior to testing.

Figure 6: Samples in desiccator chamber along with the deionized water.

Drierite was expected to absorb any water that permeated through the membrane, and this absorption would show up in successive weight measurements. The vials were then placed in a desiccating chamber exposed to a reservoir of deionized water, saturating the atmosphere. The vials were weighed periodically to quantify the water gain and the permeation coefficient calculated for each sample. The samples in the desiccator chamber are shown in Figure 6.

In addition to evaluating unstretched elastomers, it was desired to understand the effect of pre-stretch on the permeation coefficient. The membranes were biaxially stretched to different amounts, depending on the ultimate elongation until failure shown in Table 1. The pre-stretching procedure is shown in Figure 7. An adhesive was applied to the acrylic ring to ensure that the tension from the stretched membrane would cause it to fail.

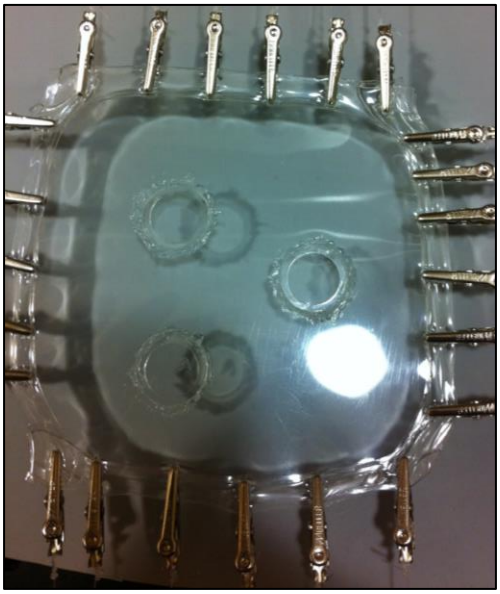

Figure 7: Mechanically pre-stretching the elastomer.

The actual percentages are presented in Table 1, and they were calculated from the before and after thicknesses of the membranes used.

Table 1: Percentages of pre-stretched applied to each membrane with 100% being original size with SG (Sylgard), BS (Bluestar), PH (phenyl), PU (polyurethane), and VHB.

SG	BS	PH	PU	VHB
102%	383%	255%	102%	256%
	433%	277%		401%
				447%

The results from the three experiments were basic weight gain measurements, which were converted into permeation coefficients. The permeation coefficients quantified how much permeant (water) was gained during a set amount of time. The calculations accounted for the membrane thickness, pressure drop across the membrane, and the membrane surface area [12]:

$$P = \frac{(quantity\ of\ permeant)(thickness)}{(area)(time)(pressure\ drop)} \quad (1)$$

The results from the pre-stretch data were unexpected because all samples repeatedly showed a much larger permeation coefficient when pre-stretched. It was initially hypothesized the pre-stretched samples would show a much lower permeation coefficient than the regular samples. Unstretched, cross-linked PDMS is an array of randomly positioned linear chains and these chains were presumed to become elongated with stretching, causing the vacancies to close or reduce as shown in Figure 8 [13].

(a) 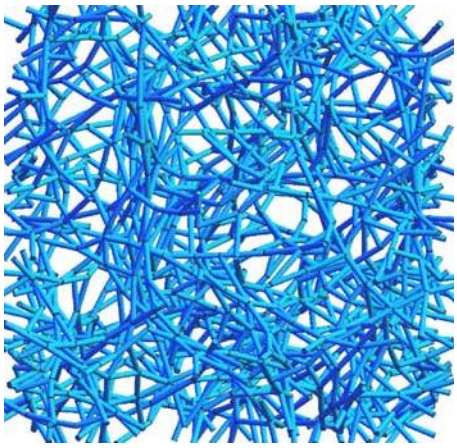 (b) 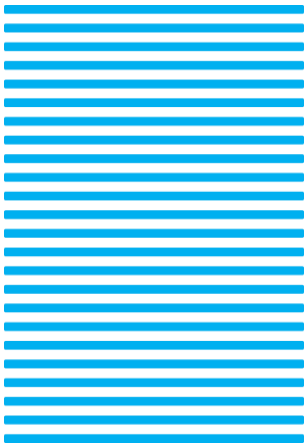

Figure 9: Hypothesized Effect of Pre-Stretch on PDMS: (a) PDMS before any stretching, (b) PDMS after stretching.

However, this was not observed via data analysis. Figure 10 demonstrates the difference in permeation coefficients between pre-stretched samples and unstretched samples. The data consistently showed the pre-stretched samples had higher permeation coefficients than the unstretched samples.

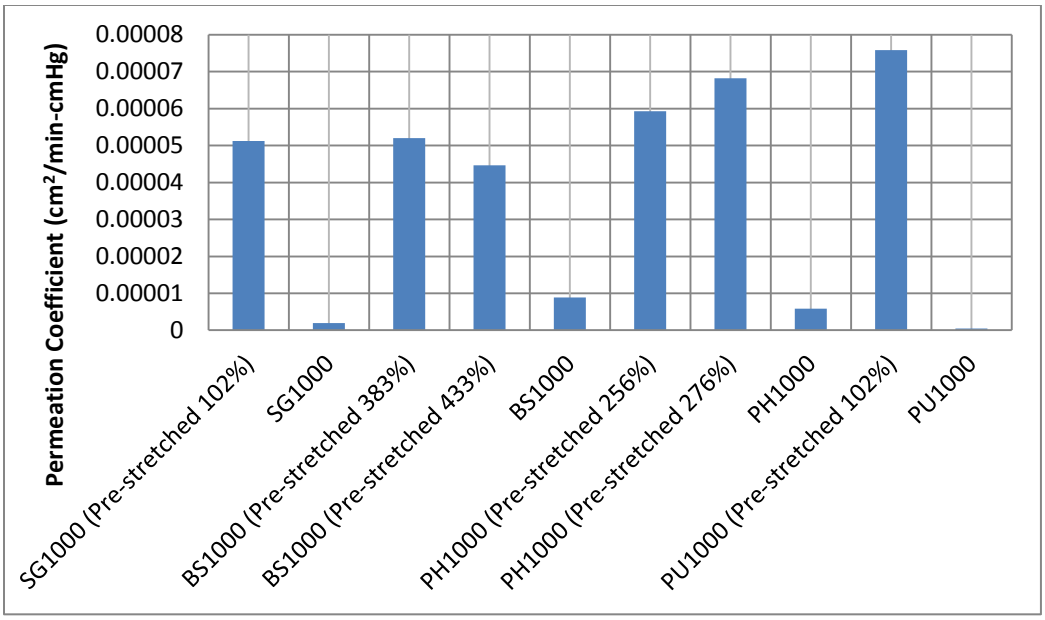

Figure 10: Pre-stretched samples versus normal samples of PDMS.

These results suggest that instead of the vacancies being reduced, they must grow (or connect with each other) to account for the increase in the permeation coefficient.

Permeation Definition via Diffusivity

Experimental research focused on the topic of permeation of water through PDMS, instead of the diffusion coefficient. Permeation is the rate by which a gas or vapor passes through a polymer, and it occurs in three steps. The first step involves the absorption of the permeating substance into the polymer just at the boundary of the polymer's face. The second step is the diffusion of the permeant through the thickness of the polymer until it reaches the other side. The last step is the evaporation or desorption of the permeant from the surface of the polymer. Absorption and desorption of the permeating species is typically quicker than the second step for water, making diffusion the time-limiting step. For diffusion to take place, there are two vital features the polymer must possess: free

volume and continuous path. Free volume is necessary because the permeating species must pass through the polymer by traveling via vacancies in the polymer. A continuous path through the polymer is important because if the vacancies ceased to exist after a certain point in the membrane, the permeating species would also stop because it cannot move. This is represented in Figure 11.

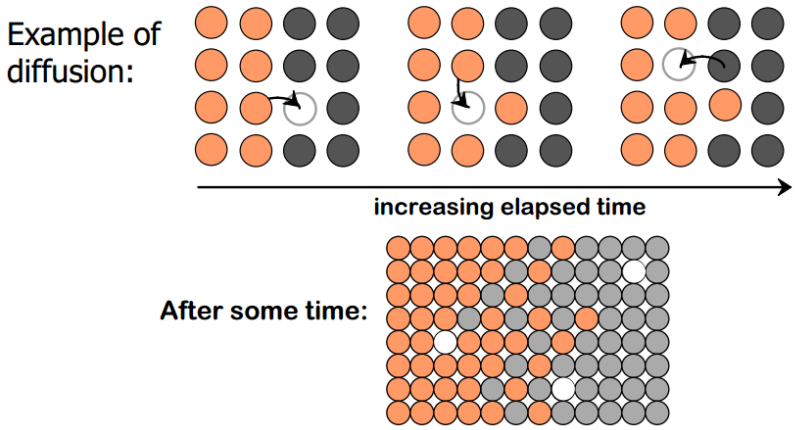

Figure 11: Diffusion through a molecular system.

The focus of the modeling research is to study diffusion since it is the time-limiting step for water permeation through PDMS. The permeation coefficient is related to the diffusion coefficient via a solubility coefficient:

$$P = D * S \tag{2}$$

The permeation coefficient is calculated using Equation 1, and the solubility coefficient is the volume of vapor at standard temperature and pressure per unit volume of polymer per unit pressure. The solubility coefficient is hypothesized to be constant for each type of

PDMS (Sylgard, Bluestar, and Phenyl), and stretching the sample does not change any variable in the solubility coefficient calculation, leaving the diffusion coefficient the only other variable in Equation 2 that must increase for the permeation coefficient to increase. However, by analyzing the change of the diffusion coefficient via molecular dynamics, it might be proven that the solubility does not remain constant and varies with different properties of the permeating species or PDMS [14].

Computational Research

Molecular Dynamics History

Molecular dynamics was introduced by Alder and Wainwright in the late 1950s to study hard spheres. Through their study, new behaviors of simple liquids were observed. It was not until 1964 that Rahman carried out the first simulation using a realistic potential for liquid argon. Rahman and Stillinger were the first to run a molecular dynamics simulation of liquid water in 1974. From 1974 to now, molecular dynamics simulations have greatly expanded to all realms of research. Molecular dynamics has been found to be extremely useful in studying biological molecules such as solvated proteins, protein-DNA complexes, and ligand binding. However, other frontiers in which molecular dynamics have been incorporated are mixed quantum mechanical-classical simulations that are being utilized to analyze surface potentials, NMR structures, and X-ray crystallography [15].

Classical Mechanics

In this branch of molecular dynamics simulation, Newton's second law, $F=ma$, is used to analyze molecules. The force acting on the particle, F, is equal to the particle's mass, m,

multiplied by its acceleration, a. Based on the knowledge of a particles mass and the forces acting upon it, the acceleration of each particle can be determined. This translates to the positions, velocities, and accelerations of the particles, and this can be turned into average values of many properties such as kinetic energy, diffusion coefficients, and thermodynamic properties. Another advantage of classical mechanics is that it is deterministic, meaning that after the positions and velocities of all the particles are determined, the state of the whole system can be determined for any time [15]. The molecular dynamics code LAMMPS is the program used in this project [16].

Computing Diffusion Coefficients

Molecules collide with themselves, other particles within a system, and a system's boundaries (if the boundaries are rigid). The trajectory that any one molecule or particle takes during a given time period is both erratic and unpredictable [17]. Whether the molecules are of a solid, liquid, or gas, they all vibrate and have a trajectory unless at absolute zero, but diffusion of water through PDMS would be futile at that temperature [18]. A particle's path through a medium is difficult to continuously determine, but the distance the particle has travelled can be quantified via the mean-square displacement of the particle (MSD). The MSD is a measure of the average distance a molecule travels, and it is defined as the following:

$$MSD(t) = \langle \Delta \mathbf{r}_i(t)^2 \rangle = \langle \left(\mathbf{r}_i(t) - \mathbf{r}_i(0) \right)^2 \rangle \quad (3)$$

In Equation 3, the quantity within the parentheses, $\mathbf{r}_i(t) - \mathbf{r}_i(0)$ is the vector displacement a molecule *i* has traveled over some time *t*. Notice, that only the vector location of a particle at the beginning of time, *t*=0, and at a "snapshot" or specified time, *t*=t, is needed to compute the MSD of the particle. The quantity is squared and averaged as noted by the angle brackets surrounding the term [17]. The limitation in Equation 3 arises in the fact that it only measures the MSD for one particle. A more comprehensive equation is needed to accurately measure a bulk of water molecules, and this is done by averaging the MSD over all particles in a particular system [19]. All that is needed is to sum the MSD for all particles from *i* to *N*, and then divide by *N*:

$$MSD(t) = \sum_{i=1}^{N} \frac{\langle \Delta \mathbf{r}_i(t)^2 \rangle = \langle \left(\mathbf{r}_i(t) - \mathbf{r}_i(0)\right)^2 \rangle}{N} \tag{4}$$

The MSD by itself does not offer any insight into diffusivity, but the plot of MSD versus time yields the derivative of MSD. A sample MSD plot is shown in Figure 12.

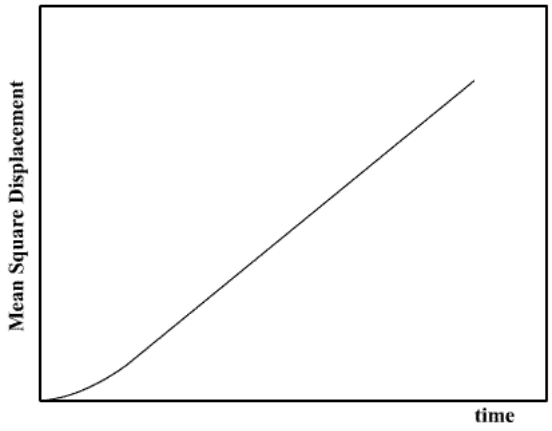

Figure 12: Example mean squared displacement plot.

The linear relationship between MSD and time is observable which means that as time increases the distance a particle travels increases in proportion to a slope [20]. However, Figure 12 is an approximation because it is averaged over a long period of time. During short intervals, the MSD plot is nonlinear because the penetrant has not collided with a sufficient number of other molecules in the system to provide an averaged measure of its diffusive motion. This nonlinear data is ignored in the calculation of the diffusion coefficient. Also, MSD for a solid system (frozen water) reaches a finite value, but MSD for a liquid or gas grows linearly with time. The slope of Figure 12 is used to calculate the diffusion coefficient, *D*, of a diffusing species in a medium. The equation is the following:

$$D = \lim_{t\to\infty} \frac{1}{2dt} \langle \left(\mathbf{r}_i(t) - \mathbf{r}_i(0)\right)^2 \rangle \tag{5}$$

The *d* in Equation 5 is the number of dimensions of the system. For the case of water through PDMS it will be 3 since the system will be a three-dimensional volume of water and PDMS [21]. From the diffusion coefficient, the time-independent D_o and activation energy can be found using the Arrhenius relationship:

$$D = D_0 \, e^{-E_a/RT} \tag{6}$$

The variable *R* represents the gas constant (8.31 J/mol-K or 8.62×10^{-5} eV/atom-K), and *T* is the absolute temperature in K. Equation 6 can be rewritten using natural logarithms:

$$\ln D = \ln D_0 - \frac{E_a}{R}\left(\frac{1}{T}\right) \quad (7)$$

Equation 7 leads to the calculation of the time-independent pre-exponential and the activation energy because it is in the slope-intercept format of a line. A plot of ln *D* versus the reciprocal of the independent variable *T* will lead to a slope of the best-fit line. The slope is equal to the activation energy divided by the gas constant, or rearranged:

$$E_a = -(slope)R \quad (8)$$

The y-intercept of the best-fit line is equal to ln D_0 or,

$$D_o = e^{y-intercept} \quad (9)$$

The diffusion of water through PDMS will not only be tested at room temperature (300K), but also at 200K and 400K to study the activation energy and time-independent pre-exponential [15].

Experimental Setup

Coarse-Grained Water Model

In order to accurately study diffusion of water through PDMS, water molecules must be added to a system of PDMS at random [22]. A problem arises in LAMMPS because the random command to create atoms is only capable of creating single atoms at random coordinates, not molecules [23]. The advantage of using the *create_atoms* command is that it creates atoms in a way that models diffusion behavior, but water consists of three atoms,

two hydrogen atoms and one oxygen atom. The task was to create a coarse-grained (CG) water model that mimics the properties and behavior of water but can be encompassed into a molecular "atom." The advantage in using a CG model for water is that it is less computationally expensive and can be applied to larger systems. However, CG models require CG force fields in atomistic simulations. It was easy to create a molecular atom that represents a water molecule by changing the mass of the CG model, but the force field to correlate the CG water model to a water molecule was the crucial aspect [24].

A literature search was made to find any such models that were previously used to model water as a molecular atom. The most closely related model employed the MARTINI force field which uses one CG bead to describe four water molecules (atomic mass = 72 g/mol). However, with this force field, using the 12-6 Lennard-Jones potential produced a poor representation of water properties and behavior. To improve the MARTINI force field, different potentials were utilized to match the properties between the CG bead and water molecules [25]. Chiu et al. were able to closely match the CG bead properties to those of water, and the Morse potential was used in their research. In the paper, they noted the Morse potential has the form:

$$V_M(r) = \varepsilon\left[e^{\alpha\left(1-\frac{r}{R_0}\right)} - 2e^{\frac{1}{2}\left(\alpha\left(1-\frac{r}{R_0}\right)\right)}\right] \tag{10}$$

In Equation 10, energy is minimized at R_0 which is the equilibrium bond distance, ε is the bond dissociation energy, and r is a parameter that measures the curvature of the potential

around R_0. The value of α governs the compressibility of the CG model. The parameters used by Chiu et al. that accurately model water are presented in Table 2.

Table 2: Morse potential parameters for the CG water (W4) [25].

Interaction Site	α	ε (kJ/mol)	R_0 (nm)	Atomic Mass (g/mol)
W4	7	3.4	0.629	72.062

This was then taken into LAMMPS to correlate the literature parameters to those for LAMMPS software, with the important parameters only being those associated with the CG water (W4). In LAMMPS, the *pair_style* command dictates the potential used in a given simulation. In this case, the command would have *morse* following the command to signify which potential will be used, followed by the parameters in the correct LAMMPS units. LAMMPS shows the Morse potential to have the form:

$$E = D_0\left[e^{-2\alpha(r-r_0)} - 2e^{-\alpha(r-r_0)}\right] \qquad r < r_c \tag{11}$$

Equation 11 and Equation 10 are similar but not exact as they should be for the parameters to hold true in LAMMPS [27]. The difference between the two equations is in the value of α because in Equation 10, α is unit-less, whereas in Equation 11, α has dimensions of 1/(length). To solve for α of Equation 11 in terms of α of Equation 10, Equation 10 must be rewritten so that α is replaced with β

$$V_M(r) = \varepsilon\left[e^{\beta\left(1-\frac{r}{R_0}\right)} - 2e^{\frac{1}{2}\left(\beta\left(1-\frac{r}{R_0}\right)\right)}\right] \tag{12}$$

Now, α and β can be related by equation the exponents of the exponentials and solving for α, with $R_0 = r_0$.

$$-2\alpha(r - r_0) = \beta\left(1 - \frac{r}{R_0}\right) \tag{13}$$

leading to

$$\alpha = \frac{\beta}{2r_0} \tag{14}$$

For the molecular simulations, the units of *real* were used in LAMMPS which specified a set unit for a quantity as shown in Table 3.

Table 3: Units associated with *real* units in LAMMPS [28].

Quantity	Units
mass	grams/mole (g/mol)
distance	Angstroms (Å)
time	femtoseconds (fs)
energy	Kcal/mole (Kcal/mol)
velocity	Angstroms/femtosecond (Å/fs)
force	Kcal/mole-Angstrom (Kcal/mol-Å)
torque	Kcal/mole (Kcal/mol)
temperature	Kelvin (K)
pressure	atmospheres (atm)
dynamic viscosity	Poise
charge	multiple of electron charge (1.0 is a proton)
dipole	charge*Angstroms (charge*Å)
electric field	volts/Angstrom (V/Å)
density	gram/cm^3 (g/ cm^3)

After converting the units of the parameters from Table 2 into the correct LAMMPS units, and applying Equation 14, the correct LAMMPS parameters for the CG water model were obtained as shown in Table 4.

Table 4: LAMMPS parameters for the CG water model.

Interaction Site	*pair_style* Potential	D_0 (Kcal/mol)	α ($Å^{-1}$)	R_0 (Å)
W4 (H_2O-H_2O)	*morse*	0.8126	0.5564	6.29

These parameters were implemented into the *pair_style* command according to the LAMMPS format. In order to make sure the model was an accurate depiction of water at room temperature, a sample molecular simulation was run. The results were imported into Ovito, an atomistic simulation viewer, to see if the result was in fact water [29].

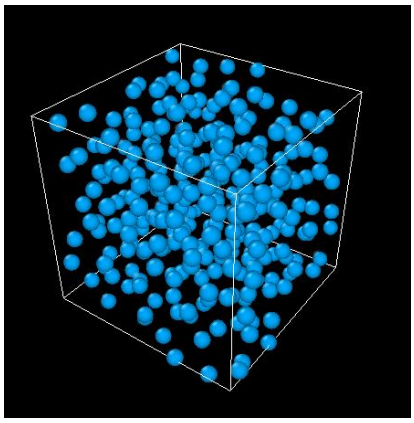

Figure 13: Screenshot of the CG water model created in LAMMPS.

Figure 13 essentially shows a volume filled with liquid water, and from the data, the density was calculated to be 0.995 g/cm^3 which is proof that the model was correctly transposed from the Chiu et al. paper into LAMMPS format and it provides a reasonable model for water.

PDMS-Water and PDMS-PDMS Interactions

Polydimethylsiloxane is composed of methyl groups (CH_3), silicone (Si), and oxygen (O), and in all experiments, the PDMS in the system will consist of 10 chains, each 679 units long. The atomic mass of one chain is approximately 50,512.9 g/mol. Just as water

interacts with itself during diffusion, water interacts with PDMS via water-CH_3, water-Si, and water-O interactions, and these are all important to account for when developing an accurate LAMMPS model to study diffusion of water through PDMS. Thus, correct *pair_style* potentials must be associated with each of these interactions to provide accurate representations. This was done by first plotting Equation 11 against a range of *r* values to obtain the curve of the Morse potential and then assessing the necessary values to implement into a standard Lennard-Jones potential to match the curve of the Morse potential. The Lennard-Jones potential used in LAMMPS, named *lj/cut*, takes the form

$$E = 4\varepsilon\left[\left(\frac{\sigma}{r}\right)^{12} - \left(\frac{\sigma}{r}\right)^{6}\right] \qquad r < r_c \tag{14}$$

Equation 14 was plotted using the same range of *r*, but ε was the same value as D_0 and σ was the close to the value of r_0 from Equation 11. When Equation 11 and 14 were plotted with these parameters, they showed to provide a good approximation [30]. Using the values for ε and σ and the Lorentz-Berthelot equations, the ε and σ for the water-PDMS interactions can be calculated. The Lorentz-Berthelot mixing equations are the following [31]:

$$\sigma_{ij} = \frac{\sigma_{ii}+\sigma_{jj}}{2} \tag{15}$$

and

$$\varepsilon_{ij} = \sqrt{\varepsilon_{ii}\varepsilon_{jj}} \tag{16}$$

The following table shows all the parameters used for water-methyl, water-silcone, and water-oxygen interaction sites.

Table 5: Parameters and potentials used for interactions between H_2O-PDMS.

Interaction Site	*pair_style* Potential	ε (Kcal/mol)	σ (Kcal/mol)
H_2O-Si	*lj/cut*	0.323728	4.67
H_2O-O	*lj/cut*	0.252982	4.18
H_2O-CH_3	*lj/cut*	0.394360	4.39

For the 6 different interaction sites of PDMS-PDMS, the parameters were provided from literature. Frischknecht and Curro studied and improved the united atom force field for PDMS. They used a potential that was called the "explicit atom class II model" potential, and this was a term specified by them to describe the different interaction parameters that need to be implemented to model PDMS accurately [32].

Table 6: Parameters and potentials used for interactions between PDMS-PDMS [32].

Interaction Site	*pair_style* Potential	ε (Kcal/mol)	σ (Kcal/mol)
Si-Si	*lj/class2/coul/cut*	0.1310	4.29
Si-O	*lj/class2/coul/cut*	0.0772	3.94
Si-CH_3	*lj/cut/coul/cut*	0.1596	3.83
O-O	*lj/class2/coul/cut*	0.0800	3.30
O-CH_3	*lj/cut/coul/cut*	0.1247	3.38
CH_3-CH_3	*lj/cut/coul/cut*	0.1944	3.73

Cross-Linked PDMS versus Not Cross-Linked PDMS

The PDMS that is used in these simulations is not cross-linked, but the data obtained can still provide insight into diffusion of water through cross-linked PDMS. The basic definition of diffusion that was shown in Figure 11 remains the same whether PDMS is cross-linked or not; water diffusion takes place through the vacancies in the polymer. Regardless of the amount of cross-linking, water diffusion can be studied and generalized to be applied to structurally-different PDMS systems. A key point to make is that both cross-linking and chain length affect the viscosity of PDMS. The simulation models in this

work have a very high molecular weight, which means that they would effectively be elastomers due to molecule entanglements (solid-like). Thus, the computation model and the experimental model are related in the fact that each represents PDMS as an elastomeric solid; the experimental work achieves this through cross-linking while the simulation study achieves this via high molecular weights.

LAMMPS Simulation Procedure

All simulation codes for the experiments were structured the same way. The simulation begins by reading the results from when PDMS has reached equilibrium, and the *pair_style potentials* and all the parameters associated with the interaction sites are included. The final temperature is then set and PDMS is allowed to reach equilibrium before penetrants are added to the system. Then, the CG water model act as the penetrant, and 100 "atoms" are added to the PDMS system at random coordinates. Energy minimization takes place after the penetrants are added, and the isothermal-isobaric (npt) ensemble is used to generate positions and velocities by performing the time integration on the Nose-Hoover style non-Hamiltonian equations of motion [33]. The MSD is computed 10 times to obtain 10 sets of data.

Procedure

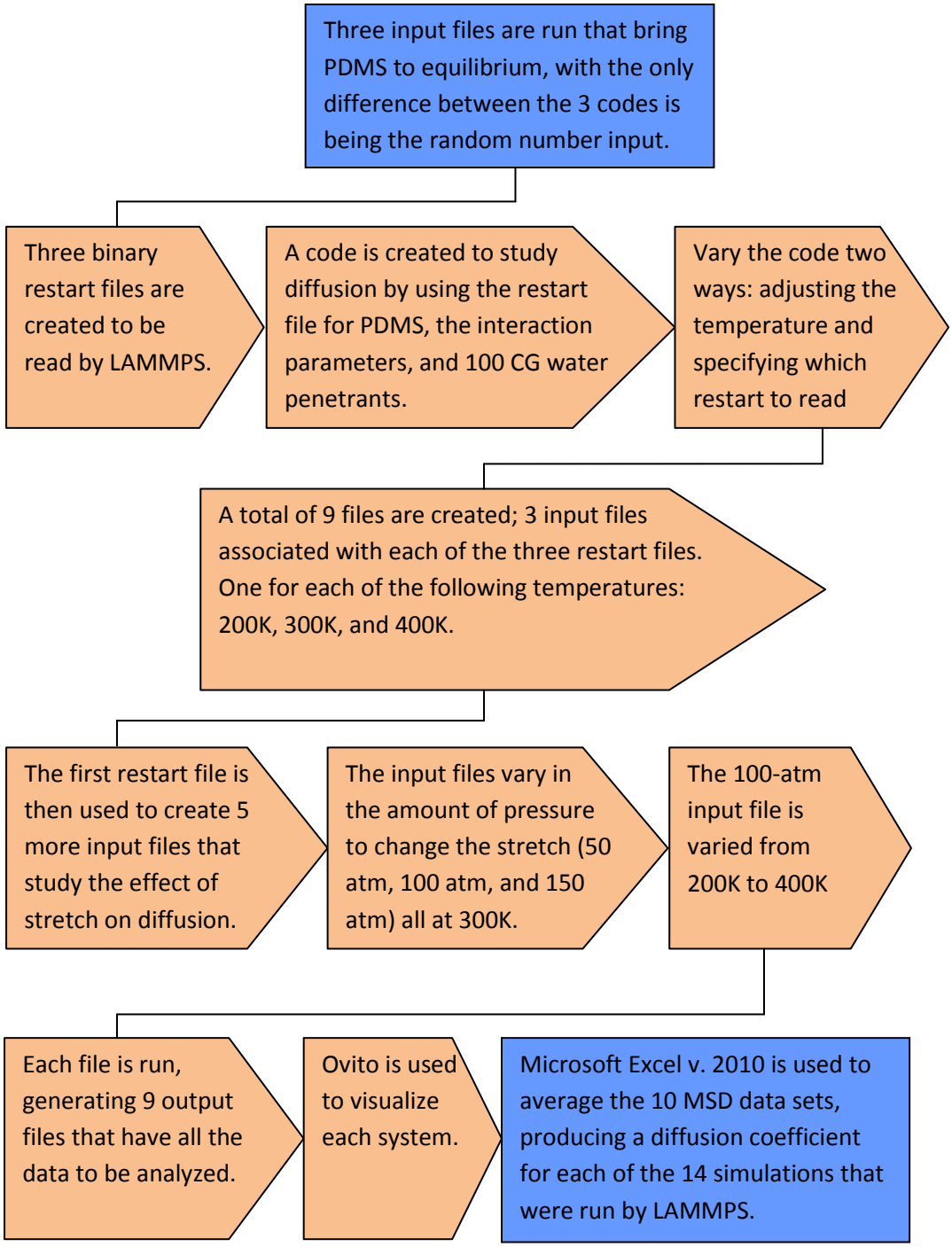
Three input files are run that bring PDMS to equilibrium, with the only difference between the 3 codes is being the random number input.
Three binary restart files are created to be read by LAMMPS.
A code is created to study diffusion by using the restart file for PDMS, the interaction parameters, and 100 CG water penetrants.
Vary the code two ways: adjusting the temperature and specifying which restart to read
A total of 9 files are created; 3 input files associated with each of the three restart files. One for each of the following temperatures: 200K, 300K, and 400K.
The first restart file is then used to create 5 more input files that study the effect of stretch on diffusion.
The input files vary in the amount of pressure to change the stretch (50 atm, 100 atm, and 150 atm) all at 300K.
The 100-atm input file is varied from 200K to 400K
Each file is run, generating 9 output files that have all the data to be analyzed.
Ovito is used to visualize each system.
Microsoft Excel v. 2010 is used to average the 10 MSD data sets, producing a diffusion coefficient for each of the 14 simulations that were run by LAMMPS.

Results and Discussion

Temperature-Varied Results with Standard Pressure (No Stretch)

The initial results are visualized using Ovito to see how the system behaves over the duration of time that the simulation runs. An Ovito snapshot of the output file from running the first restart file at 200K is shown in the following figure.

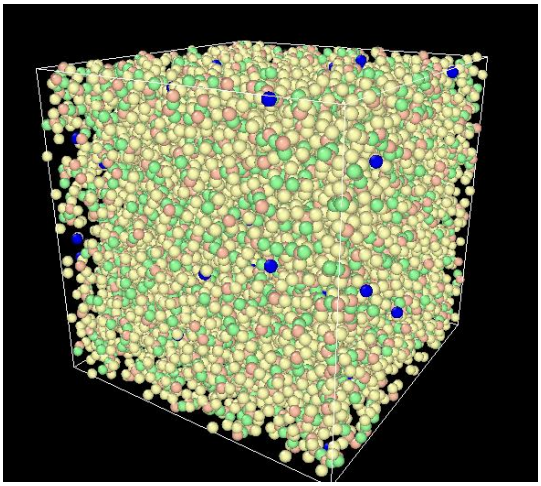

Figure 14: Ovito is used to visualize the PDMS and H_2O system. Water molecules are shown in blue.

In Figure 14, the dark blue spheres represent water, the light pink spheres represent silicon, the light green spheres represent oxygen, and the light yellow spheres represent methyl. There are 10 PDMS chains within the box, creating a filled volume. The random water molecules are added as CG models at random coordinates, as mentioned before.

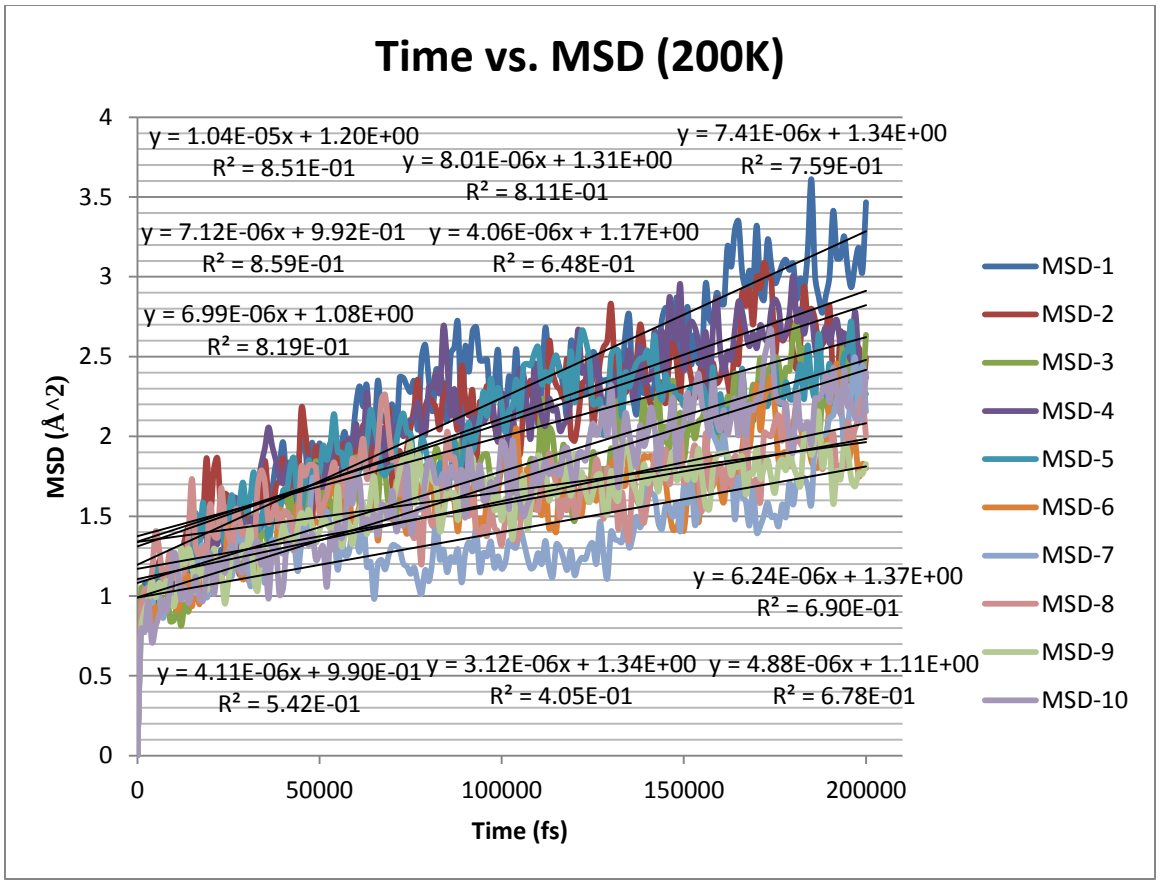

Figure 15: The 10 plots of MSD versus time for diffusion at a temperature of 200 K.

The water MSD data that is produced by the 10 data acquisition stages in the LAMMPS code are compiled using Excel and used to compute the diffusion coefficient for that particular temperature in two different ways. One way is to graph each MSD data set versus time to obtain a slope, resulting in 10 slopes that would be averaged to yield a final slope of the water MSD in the system. Using Equation 5, the final slope is divided by 6, because it is a 3-dimensional system, and converted to the appropriate diffusion units. The second way to average the data into one final slope is to average the data from the 10 data sets into one set and plot this against time. From there, a final slope is obtained, divided by 6, converted to appropriate units, and turned into a diffusion coefficient. A sample graph of

the 10 slopes and the process leading to a final slope is shown in Figure 15 for the first restart input file at a temperature of 200K. The slopes are averaged and then converted into the correct units, as shown in Table 7.

Table 7: Average slopes converted into a diffusion coefficient.

AVG Slope	[D] ($Å^2$/fs)	[D] (m^2/s)
6.23E-06	1.04E-06	1.04E-11

It was possible to record to two significant digits because Excel was instructed accordingly, and two significant digits were sufficient to describe the diffusion coefficient. The beginning data values were observed to skew the slope of each line, so the first 19,000 fs were excluded from the graphs and the process was repeated to obtain a more accurate slope and diffusion coefficient.

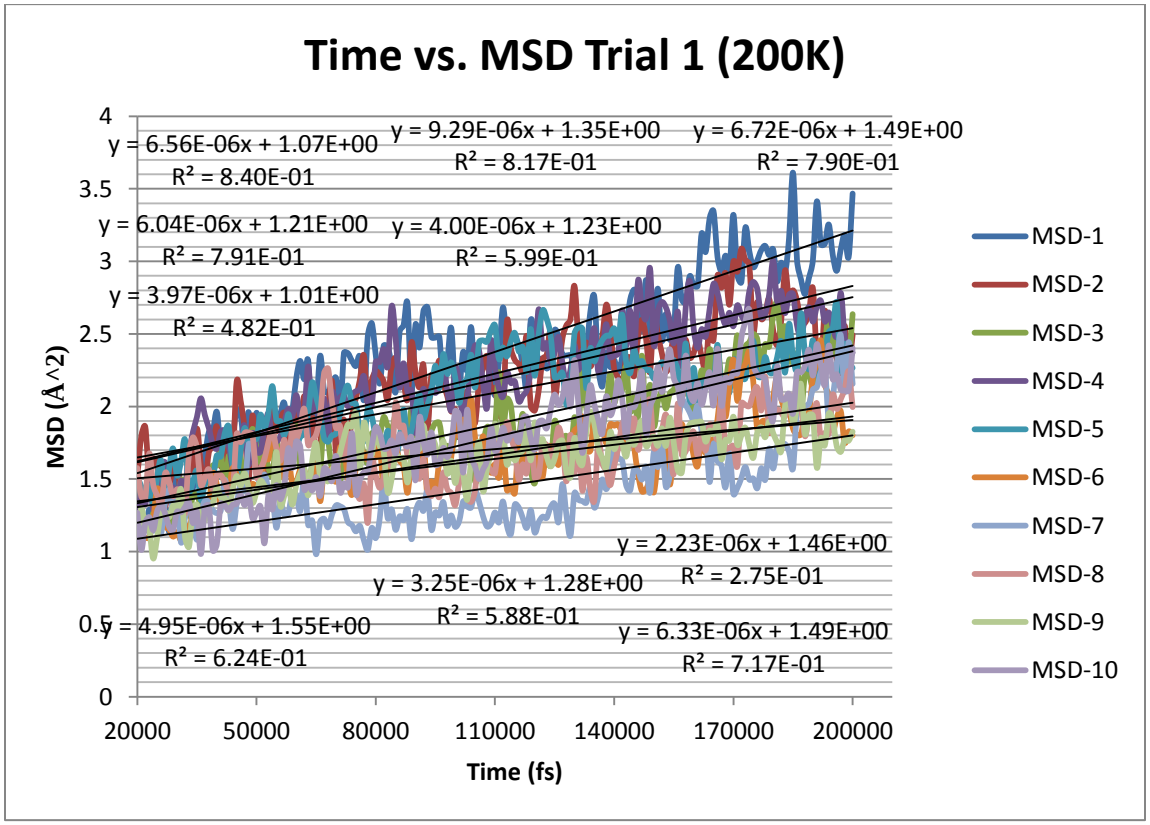

Figure 16: The 10 plots of MSD versus time for diffusion at a temperature of 200 K without the initial data.

Table 8: Averaged slopes converted into a diffusion coefficient.

AVG Slope	[D] ($Å^2$/fs)	[D] (m^2/s)
5.33E-06	8.89E-07	8.89E-12

The slopes did show a change when the outliers were removed from the data sets as shown in Figure 16 and Table 8. Figure 16 will be the way data is presented in the rest of this paper due to its simplicity, but the slopes and diffusion coefficients will be presented from both calculations. The plots for the data with the outliers will be excluded due to the skewed slopes that they yield leading to poor diffusion coefficients.

The second way yielded results that were the same in some cases and close in others. An example of averaging the data first and then plotting it against time is shown in Figure 17.

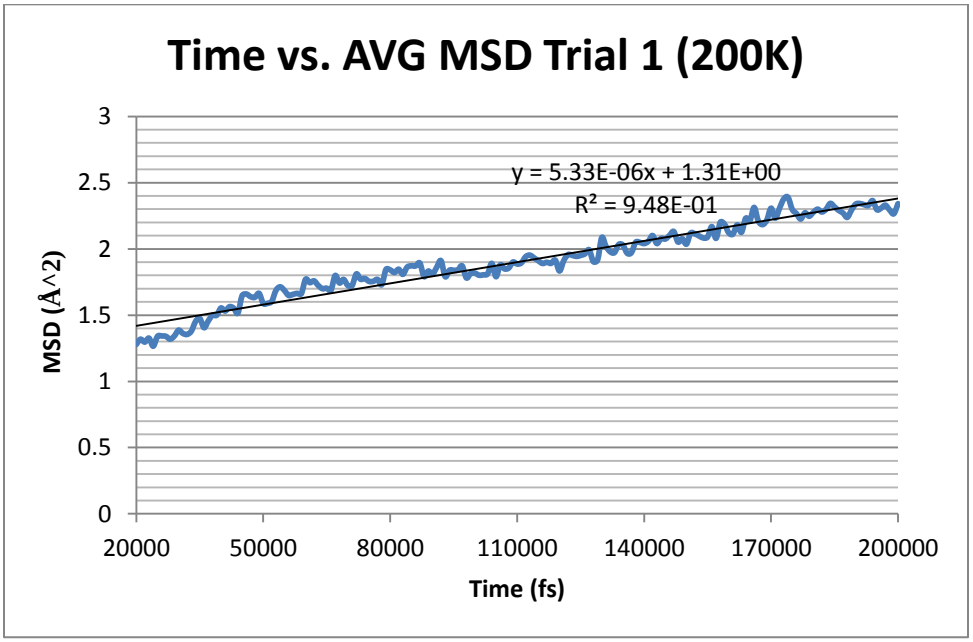

Figure 17: MSD versus time after the 10 sets of data have been averaged.

The slope is then transformed into a diffusion coefficient in the same way.

Table 9: The slope is used to calculate a diffusion coefficient.

AVG Slope	[D] ($Å^2$/fs)	[D] (m^2/s)
5.33E-06	8.88E-07	8.88E-12

Each of the three restart input files was used to study water diffusion through PDMS at three different temperatures: 200K, 300K, and 400K. For simplicity, the method to compute the slopes was to average the data before plotting. The next three figures show each trial at the three different temperatures.

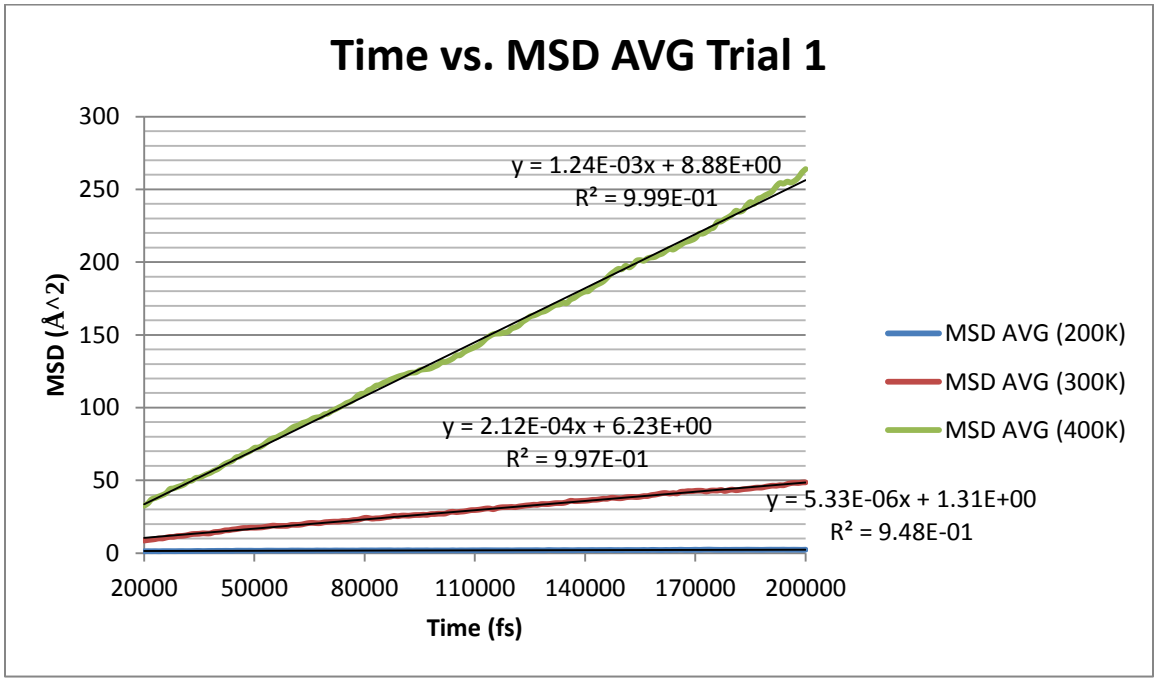

Figure 18: Plot of MSD versus time after the 10 sets of data from trial 1 have been averaged for 200K, 300K and 400K.

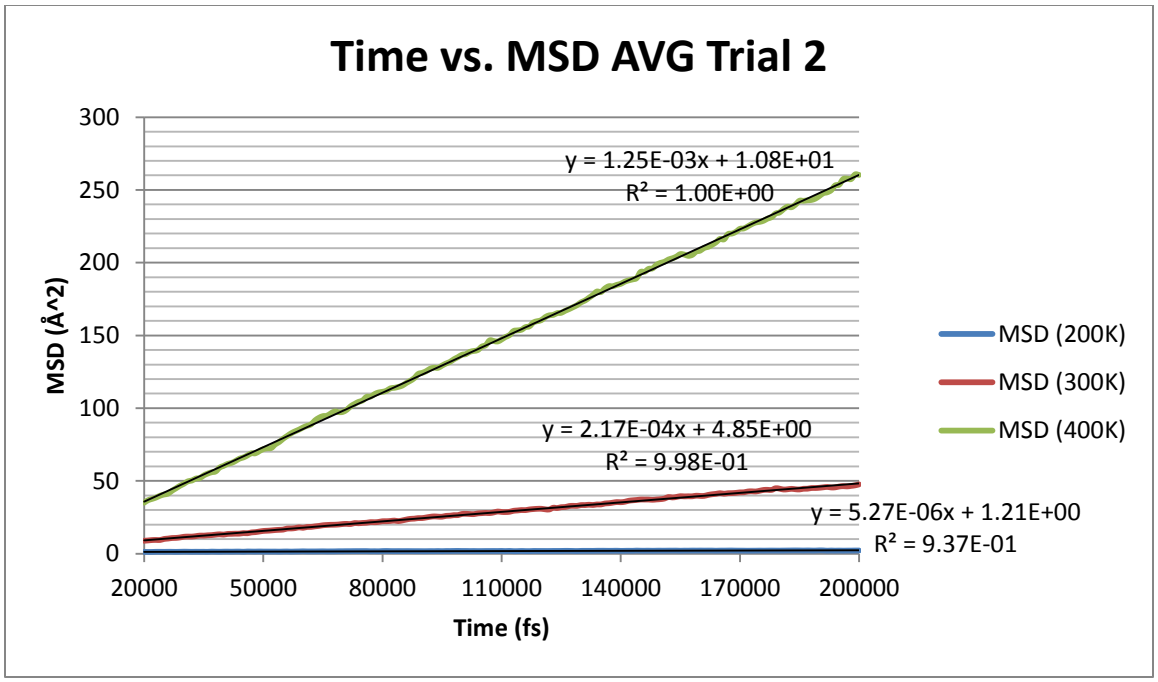

Figure 19: The graph shows the plot of MSD versus time after the 10 sets of data from trial 2 have been averaged for 200K, 300K and 400K.

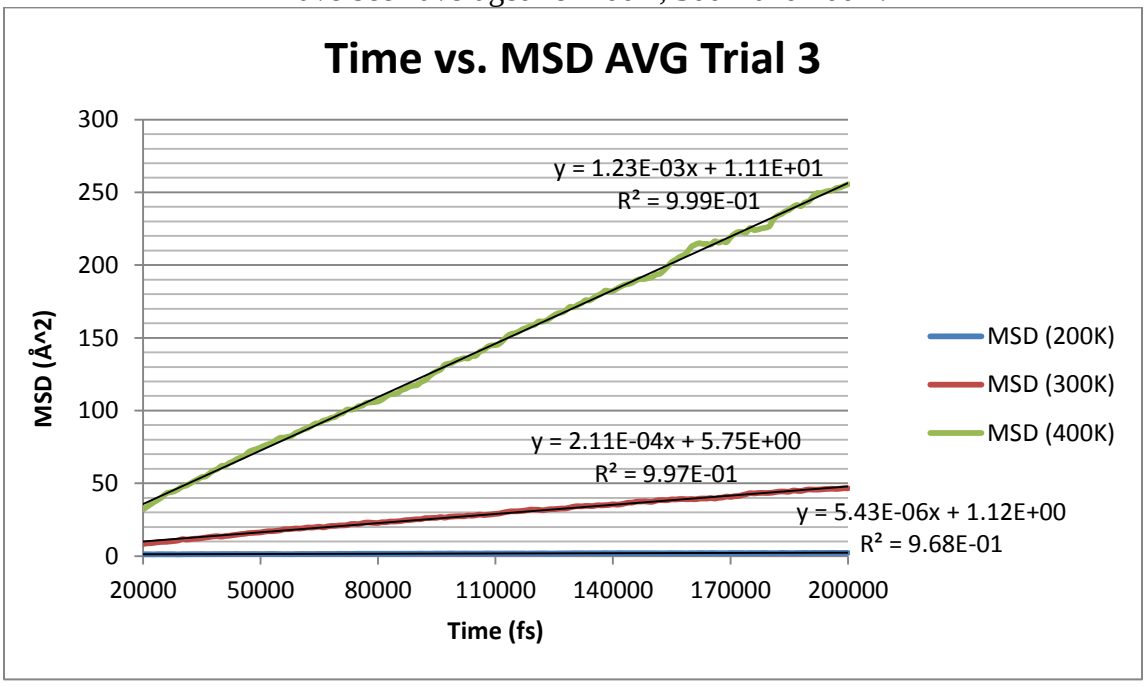

Figure 20: The graph shows the plot of MSD versus time after the 10 sets of data from trial 3 have been averaged for 200K, 300K and 400K.

The slopes from these nine lines were used to calculate nine diffusion coefficients. The experiments were repeated to ensure the repeatability of the data. The following table shows the final data from temperature variation at atmospheric pressure.

Table 10: The slopes and diffusion coefficients showing the role of temperature.

Trial 1				
Temperature (K)	**Slope**	**AVG Slope**	**[D] (Å^2/fs)**	**[D] (m^2/s)**
200	5.33E-06	5.33E-06	8.88E-07	8.88E-12
300	2.12E-04	2.12E-04	3.53E-05	3.53E-10
400	1.24E-03	1.24E-03	2.07E-04	2.07E-09
Trial 2				
Temperature (K)	**Slope**	**AVG Slope**	**[D] (Å^2/fs)**	**[D] (m^2/s)**
200	5.27E-06	5.27E-06	8.78E-07	8.78E-12
300	2.17E-04	2.17E-04	3.62E-05	3.62E-10
400	1.25E-03	1.25E-03	2.08E-04	2.08E-09
Trial 3				
Temperature (K)	**Slope**	**AVG Slope**	**[D] (Å^2/fs)**	**[D] (m^2/s)**
200	5.43E-06	5.43E-06	9.05E-07	9.05E-12
300	2.11E-04	2.11E-04	3.52E-05	3.52E-10
400	1.23E-03	1.23E-03	2.05E-04	2.05E-09

The diffusion coefficient was calculated under the same conditions for three trials because the deviation from one data set to the other was to be assessed. Table 11 below shows the same data as Table 10, but it shows the calculated average diffusion coefficient at each temperature and the standard deviation of each value.

Table 11: The average diffusion coefficient for each temperature along with the standard deviation of each coefficient.

[D] (m^2/s)			
	Temperature (K)		
Trial	200	300	400
1	8.90E-12	3.53E-10	2.07E-09
2	8.80E-12	3.62E-10	2.08E-09
3	9.10E-12	3.52E-10	2.05E-09
AVG	8.91E-12	3.56E-10	2.07E-09
STDEV	0.13E-12	0.05E-10	0.02E-09

Using the slopes at the different temperatures for each restart file, the activation energy, E_a, and the time-independent pre-exponential were calculated. Only the plot of the first set of data from the first restart file will be shown because the other two resemble this one almost exactly. Equations 7-9 led to the following plot.

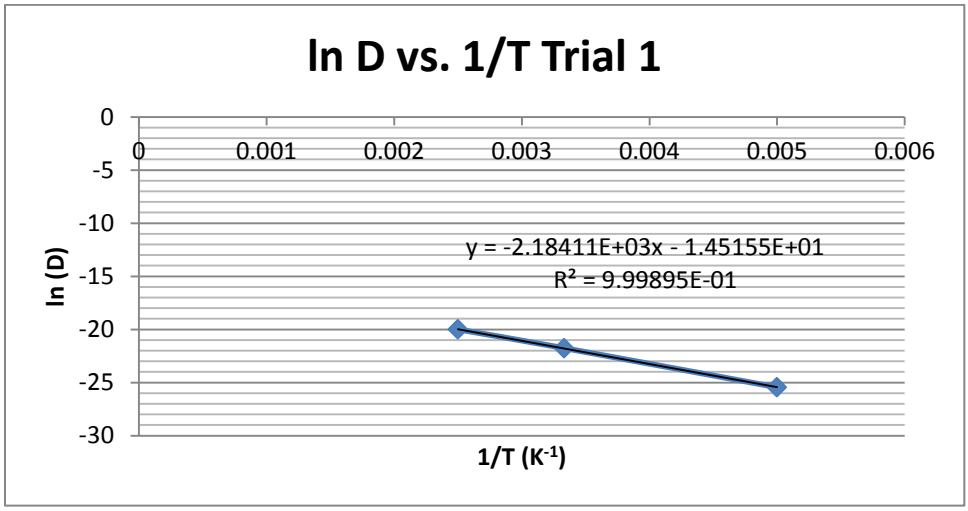

Figure 21: Plot of ln (D) versus 1/T.

The slope of this line was used to calculate E_a, and the y-intercept was used to calculate D_0. The table below shows E_a and D_0 for each trial, along with the average value and standard deviation of each value.

Table 12: Computed values for E_a and D_0 for each trial, its average and the standard deviation.

	Trial 1	Trial 2	Trial 3	AVG	STDEV
E_a (Kcal/mol)	4.36	4.36	4.32	4.35	0.02
D_0 (m^2/s) x 10^{-7}	4.90	5.20	4.80	5.00	0.2

Stretch Results with Temperature Variation

The PDMS was stretched by varying the pressure in the volume containing the PDMS from 0 atm (gauge pressure), 50 atm, 100 atm, and 150 atm and maintaining a temperature of 300K. Notice that anisotropic pressure is applied to the system, meaning that the system will be under compression. Anisotropic means that a condition is not changed in the same direction, so in the x- and y- directions, a pressure was applied, but the z-direction was left alone to equilibrate the system by either elongating or shrinking. Instead of tensile strain, the system will be experiencing compressive strain due to the bi-axial pressure being applied to the PDMS-water system. The 0 atm data was already completed during the part of the experiment when no stretch was included in the simulation. The simulation that used 100 atm was then subjected to temperatures of 200K and 400K. Again, the data was plotted separately, the slopes averaged to a final slope, and the diffusion coefficient calculated, but averaging the data first and then plotting it against time is how the data will be presented. To begin, it is important to know by what percent each dimension of the system (x, y, and z) are either elongated or shrunk. The following table documents the original dimensions and the new dimensions of the simulation for each anisotropic pressure. The pressure was only applied to the x- and y-directions.

Table 13: Computed percent difference in each difference; a negative value means shrinkage, and a positive value means elongation.

Corresponding Stretch									
	Original Dimensions (Å)			Stretched Dimensions (Å)			Stretch (%)		
P (atm)	X	Y	Z	X	Y	Z	X	Y	Z
0	74.86	74.86	74.86	74.86	74.86	74.86	0.00%	0.00%	0.00%
50	74.86	74.86	74.86	71.76	69.66	83.70	-4.14%	-6.95%	11.81%
100	74.86	74.86	74.86	64.95	66.44	96.53	-13.24%	-11.25%	28.95%
150	74.86	74.86	74.86	61.20	61.72	109.81	-18.25%	-17.55%	46.69%

A sample plot of the data from running the simulation at 300K with 50 atm anisotropic is shown in the figure below.

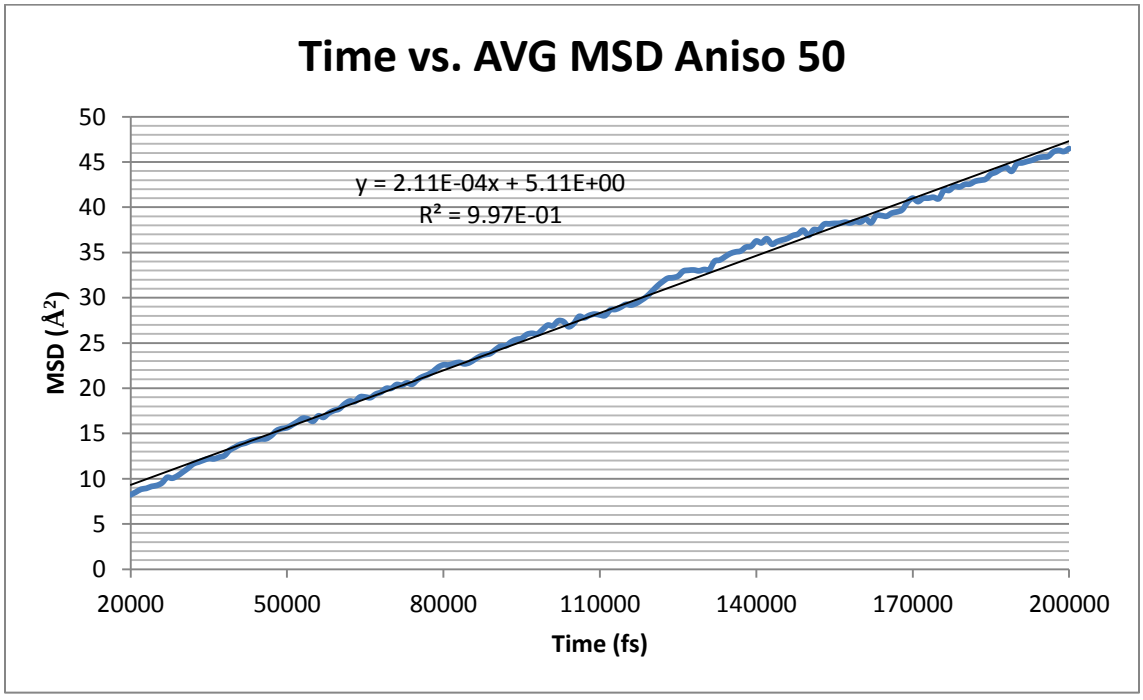

Figure 21: Plot of time versus MSD at 300K and 50 atm anisotropic pressure.

The slope is then turned into a diffusion coefficient as before. The values from the three different pressures at 300K are reported in the table below.

Table 14: Computed diffusion coefficients for each anisotropic gauge pressure.

Gauge Pressure (atm)	Slopes	AVG Slope	[D] (Å^2/fs)	[D] (m^2/s)
0	2.12E-04	2.12E-04	3.53E-05	3.53E-10
50	2.11E-04	2.11E-04	3.52E-05	3.52E-10
100	2.51E-04	2.51E-04	4.18E-05	4.18E-10
150	3.05E-04	3.05E-04	5.08E-05	5.08E-10

The simulation for 100 atm anisotropic pressure was run at 200K and 400K, and the activation energy and time-independent values were calculated.

Table 15: Computed diffusion coefficients for each temperature at 100 atm anisotropic pressure and the activation energy and time-independent pre-exponential.

Temperature Variation	
Temperature (K)	**[D] (m^2/s)**
200	8.75E-12
300	4.18E-10
400	2.40E-08
E_a (Kcal/mol)	6.05
D_0 (m^2/s)	2.66E-05

Conclusions

The experimental results showed that when a membrane is stretched, water permeation through the membrane increases. The hypothesis of vacancies being reduced due to polymer chains elongating and organizing themselves in the membrane when stretched proved false. Using molecular dynamics simulations, the diffusion coefficient of water through PDMS was analyzed to determine if diffusion was the motivation behind increased permeation.

A program called LAMMPS was used to test 9 simulations of water diffusion through PDMS. The 9 simulations were 3 sets of 3 files that had temperatures of 200K, 300K, and 400K. The data was compiled and plotted to produce 9 different slopes which were used to calculate the diffusion coefficients of water through PDMS under each

specific condition. The 200K, 300K, and 400K each had 3 results, and they were averaged to provide a final value for the diffusion coefficient. The standard deviation was included to see the variance in the data from the 3 restart files.

The purpose of varying the temperature was to not only observe the effect of temperature increase on water diffusion, but also to calculate the activation energy and time-independent pre-exponential for water diffusion through PDMS. For each restart file, there were three data points that could be plotted with the independent variable being temperature and the dependent variable being the diffusion coefficient. Plotting the natural logarithm of *D* against the reciprocal of temperature led to an equation of a line that was used to calculate E_a in Kcal/mol and D_0 in m^2/s.

Lastly, the system was put under 3 different gauge pressures at 300K to analyze the effect of strain on diffusion. This was used to prove or disprove the hypothesis that vacancies actually enlarge when the membranes used in the experimental research were stretched or compressed. Table 14 clearly disproves the hypothesis that diffusion should decrease with compression because it was thought that if the vacancies enlarge when the membranes are stretched, then they should shrink when the membrane is compressed. However, Table 14 shows the opposite to be true: as compression increased, diffusion increased. Thus, permeation of water through PDMS is not governed by diffusion nor is it the time-limiting factor of water permeation through PDMS. The other processes, absorption and desorption, must play a bigger role than diffusion if water permeation increases with tension and diffusion increases with compression. Another possible scenario that causes the hypotheses to be skewed is that the permeation cell may not have been as effective in measuring water permeation as previously thought. Water may have leaked out of the permeation cell not through the membrane, but through other pathways, causing the permeation coefficient to be inaccurate. Nevertheless, this information is useful because it shows that the current method for testing permeation was not effective. The data from both the experimental and

computational research can be used to guide the design of an improved apparatus to test water permeation through PDMS. Thus, even though this data showed conflicting results, it can be used to improve current research techniques. The data gathered from running the simulation at 200K and 400K was used to calculate the activation energy and the time-independent pre-exponential at 100 atm anisotropic pressure by the same method.

References:

1. "Polydimethylsiloxane." <http://www.photonics.byu.edu/PDMS.phtml>
2. "Silicone Rubber." <http://albright1.com/siliconerubber/>
3. "Polydimethylsiloxane." <http://www.fao.org/ag/agn/jecfa-additives/specs/Monograph1/Additive-315.pdf>
4. "Polydimethylsiloxane." <http://www.inchem.org/documents/icsc/icsc/eics0318.htm>
5. "Silicones in Medical Applications." <https://www.dowcorning.com/content/publishedlit/Chapter17.pdf>
6. Curtis, J. M.; Colas, A. Dow Corning(R) Silicone Biomaterials: History, Chemistry & Medical Applications of Silicones, In Biomaterials Science, 2nd Edition; Ratner, B. D., Ed.; Elsevier: London, UK, 2004, 80.
7. Toepke, Michael W., Beebe, David J. and David J. Beebe. "PDMS absorption of small molecules and consequences in microfluidic applications." <http://mmb.bme.wisc.edu/research/BeebePubs/Beebe%20Pubs/b612140ctoepke.pdf>
8. "Diffusion." <http://web.utk.edu/~prack/mse201/Chapter%205%20Diffusion%20.pdf>
9. Anderson, Iian A., et al. "Multi-Functional Dielectric Elastomer Artificial Muscles for Soft and Smart Machines." *Journal of Applied Physics*. 112 (2012): 041101(1)-041101(20).
10. "Dielectric Elastomer Actuators." <http://www.smela.umd.edu/polymer-actuators/dea.html>
11. Shian, Samuel, et al. "Tunable Lenses Using Transparent Dielectric Elastomer Actuators." *Optics Express*. 7 (2013): 8669-8676.
12. Shian, Samuel, et all. "Diffusion and Permeability in Polymers."
13. "Cross-Linking Polydimethylsiloxane." <http://www.uark.edu/ua/meeg/REU/2010/Symposium/LaTisha%20Isaiah.pdf>

14. “Permeation.” <http://users.encs.concordia.ca/~woodadam/GCH6101/Diffusion%20and%20permeability%20in%20polymers.pdf>
15. “Theory of Molecular Dynamics Simulations.” <http://www.ch.embnet.org/MD_tutorial/pages/MD.Part1.html>
16. “LAMMPS Molecular Dynamics Simulator.” <http://lammps.sandia.gov/>
17. “Ljmd: Background.” <http://www.etomica.org/app/modules/sites/Ljmd/Background2.html>
18. “Vibrational Modes.” <http://chemwiki.ucdavis.edu/Physical_Chemistry/Spectroscopy/Vibrational_Spectroscopy/Vibrational_Modes>
19. “Brownian Motion.” <http://www.pma.caltech.edu/~mcc/Ph127/b/Lecture15.pdf>
20. “The Mean Square Displacement.” <http://www.compsoc.man.ac.uk/~lucky/Democritus/Theory/msd.html>
21. “Mean Square Displacement.” <http://www.fisica.uniud.it/~ercolessi/md/md/node36.html>
22. “What is Diffusion?” <http://www.austincc.edu/biocr/1406/labm/ex5/prelab_5_1.htm>
23. “create_atoms command.” <http://lammps.sandia.gov/doc/create_atoms.html>
24. “The CUMULUS Coarse Graining Method: Transferable Potentials for Water and Solutes.” <http://pubs.acs.org/doi/abs/10.1021/jp201975m>
25. “Coarse-Grained Molecular Models of Water: A Review.” <http://www.ncbi.nlm.nih.gov/pmc/articles/PMC3420348/>
26. “A Coarse-Grained Model Based on Morse Potential for Water and n-Alkanes.” <file:///C:/Users/dxs027/Downloads/ct900475p%20(1).pdf>
27. “pair_style morse command.” <http://lammps.sandia.gov/doc/pair_morse.html>
28. “units command.” < http://lammps.sandia.gov/doc/units.html>
29. “Ovito-The Open Visualization Tool.” <http://www.ovito.org/>
30. “lj/cut command.” <http://lammps.sandia.gov/doc/pair_lj.html>

31. “Lennard-Jones Potential.” <http://gozips.uakron.edu/~mattice/ps674/lj.html>
32. Frischknecht, A. L., and Curro, J. G., 2003, “Improved United Atom Force Field for Poly(Dimethylsiloxane),” Macromolecules, 36, pp. 2122–2129. <http://pubs.acs.org/doi/pdf/10.1021/ma025763g>
33. “fix nvt command.” <http://lammps.sandia.gov/doc/fix_nh.html>